IIETA International Information and Engineering Technology Association
Advancing the World of Information and Engineering

Annales de Chimie - Science des Matériaux
Vol. 49, No. 4, August, 2025, pp. 415-423
Journal homepage: http://iieta.org/journals/acsm

High-Power Laser Material Processing via Numerical Simulation of Deformable Mirror-Controlled Beam Shaping

Nada A. Hadi Kareem[1*], Nada S. Ahmade[2]

[1] Department of Physics, College of Science, Nahrain University, Baghdad 32000, Iraq
[2] Department of Physics, College of Science, University of Diyala, Diyala 10001, Iraq

Corresponding Author Email: nadaahmad@uodiyala.edu.iq

https://doi.org/10.18280/acsm.490409

Received: 5 May 2025
Revised: 15 July 2025
Accepted: 21 July 2025
Available online: 31 August 2025

Keywords:
deformable mirror, laser processing, thermal stability, closed-loop control

ABSTRACT

This paper investigates the utility of dynamic beam shaping, utilizing a deformable mirror (DM), to enhance the precision and quality of high-power laser material processing. A 128-actuator DM with closed-loop proportional-integrating-derivative (PID) control was integrated into a 3-kW fiber laser machine to generate tailored beam profiles. This study aims to bridge the gap between low-power DM applications and high-power laser material processing by investigating the thermal stability, precision, and adaptability of a 128-actuator DM system under continuous 3 kW laser operation. The tests showed that using dynamically shaped beams decreased surface roughness by 25% (Ra = 0.65 µm) and micro-crack density by 60% when compared to standard Gaussian beams. The shaped beams also led to deeper surface hardening (230 µm) and smaller warmth-affected zones (45 µm). Thermal stability tests showed the DM's stability, with floor flow at or below 0.2 µm during constant 3 kW operation. Statistical information showed that shaped beams were better at reducing thermal distortions. Although there are challenges like device fee and control difficulty, this work sets up a base for adaptive laser processing, which could help industries that need micron-level precision. A Python program imitates the dynamic beam shaping by copying how a mirror surface changes shape when actuators are used, and it calculates how the changed mirror surface changes the laser beam's spatial intensity distribution. The simulation copies the mirror's reaction to actuator inputs and guesses the resulting beam profile, giving a theoretical reason for the experimental proof in this study. Important things like mirror shape, actuator setup, beam movement, and system reaction are added into the model.

1. INTRODUCTION

High-power laser fabricating (HLMP) has become a mainstay of high-quality production, allowing incision, welding, surface hardening, and additive production to be performed with a previously unseen level of control. Such processes are important for industries such as aerospace, automotive, and medical tool manufacturing, where precision and repeatability at the micron level [1] are often a requirement. As a foundation of these processes, it must be understood that ability to control the spatial and temporal distribution of the laser power is critical. This is due to the fact that the laser intensity profile ultimately dictates the heat input, molten pool dynamics, and final microstructure of the substrate. For instance, in laser cutting of chrome steel, a Gaussian beam profile may additionally result in choppy strength deposition, causing thermal distortion or microcracks, while a tailored "top-hat" profile can enhance part quality and reduce the heat-affected zone (HAZ) [2]. Despite its essential position, traditional beam-shaping strategies, including static diffractive optical elements (DOEs), constant aspheric lenses, or segment plates, are afflicted by intrinsic limitations. These static systems cannot adapt to dynamic processing conditions, along with fluctuating thermal hundreds or varying cloth reflectivity, which are ubiquitous in high-electricity applications (>1 kW) [3]. For example, thermal lensing, a phenomenon wherein lens heating alters the beam's focal length, remains a continual undertaking in non-stop-wave laser welding, frequently requiring costly hardware recalibration mid-process [4].

To overcome those obstacles, adaptive optics, specifically deformable mirrors (DMs), have garnered extensive attention. Deformable mirrors (DMs) use piezoelectric or electrostatic actuators to change their surface shape. This capability allows for adjustments to correct wavefront errors and manage beam features like intensity, focal spot size, and divergence [5]. This is helpful for high-power laser materials processing (HLMP), where quick adjustments to beam form are needed for changing between tasks like cutting and surface texturing, or for fixing substrate warping during production. Work in lower power settings (<500 W) show what DMs can do [6]. For example, reshaping the beam from Gaussian to Bessel reduced the heat-affected zone (HAZ) by 30% when laser scribing silicon. Also, study [7] used a DM to improve power delivery in laser hardening of titanium alloys, which resulted in a 15% increase in surface hardness consistency.

However, using these methods for strong structures is difficult. High densities (>1 MW/cm²) create large thermal stresses on DM substrates, leading to actuator drift, surface change, and reduced reflection [8]. The short-term thermal-mechanical link between the mirror and the laser beam, made worse by lasting contact with multi-kilowatt lasers, has not been well studied, which leaves a major gap in designing stable DM systems for industrial use. This problem is amplified by a lack of standard ways to measure DM ability under intense conditions. While computer models, like finite element analysis (FEA) of actuator response times or heat load distribution, have been suggested [9], experiments in real HLMP situations are rare. For example, current models don't consider actuator hysteresis and thermal creep under multi-kilowatt loads. These factors are important for predicting how well DMs will perform over time in industrial uses. For example, no study has measured how actuator hysteresis or thermal creep affect beam stability during fast laser cutting of metals that can withstand high temperatures. Current control methods for DMs are taken from astronomy or biomedical imaging and are not well suited for the fast feedback loops (under a millisecond) required in HLMP [10]. The low-power studies show what DMs can potentially accomplish, but their results cannot be directly applied to high-power systems because of thermal and mechanical problems. This suggests that we need a careful study of DMs in high-power settings. Solving these problems is necessary to get the most out of DMs in industrial laser systems.

This paper explores objectives to address these gaps through 3 interrelated goals. First, we develop a high-power-compatible DM system, which combines a 127-actuator piezoelectric mirror with a closed-loop control system, relying on real-time beam diagnostics from a high-speed Shack-Hartmann wave front sensor. Second, we systematically characterize the dynamic beam properties, including spatial intensity uniformity, focal shift tolerance, and thermal load behavior at operational power levels of up to three kW, using a combination of beam profiling cameras and pyroelectric sensors. Third, we investigate the responsiveness of our system by using it to laser cut 316L stainless steel, which is used routinely in surgical implants for its corrosion resistant properties. Metrics, including cut area roughness (Ra), HAZ width, and microhardness gradients, are compared with baseline motor effects from static beam shaping. By linking DM actuator dynamics with material effects, this research improves the fundamental understanding of adaptive optics in HLMP as well as outlines details for the contractor to use in developing tailored solutions for industry.

2. MATERIAL SELECTION

The company specializes in industrially applicable materials: AA 6061 aluminum alloy and 316L stainless steel, selected for his or her contrasting thermomechanical properties and considerable packages in high-precision industries.

2.1 AA 6061 aluminum alloy

Widely used in aerospace and automotive sectors because of its high energy-to-weight ratio and great thermal conductivity (167 W/m·K) [11], AA 6061 presents a unique task for laser processing. Its rapid warmness dissipation necessitates precise strength distribution to avoid localized overheating, which can result in porosity or micro-cracking. This makes it a great candidate for comparing the dynamic beam shaping's capability to mitigate thermal gradients.

2.2 316L stainless steel

Chosen for its corrosion resistance and biocompatibility, 316L is a mainstay in medical tool manufacturing and marine engineering. Its decreased thermal conductivity (16 W/m·K) compared to aluminum affects the mentioned warmness accumulation throughout laser processing, making it appropriate for reading floor hardening and HAZ control [12]. The selection of those materials is similarly justified by means of their representation of distinct fabric instructions. Non-ferrous vs. Ferrous, AA 6061 (Al-Mg-Si) and 316L (Fe-Cr-Ni-Mo) show off divergent responses to laser energy input, enabling comparative evaluation of beam shaping efficacy. Thermal Properties, the 10-fold difference in thermal conductivity among the two substances permits probing how dynamic beam shaping adapts to various warmth dissipation necessities.

Pre-processing characterization was conducted to establish baseline material properties and understand how microstructural features may influence laser processing outcomes.

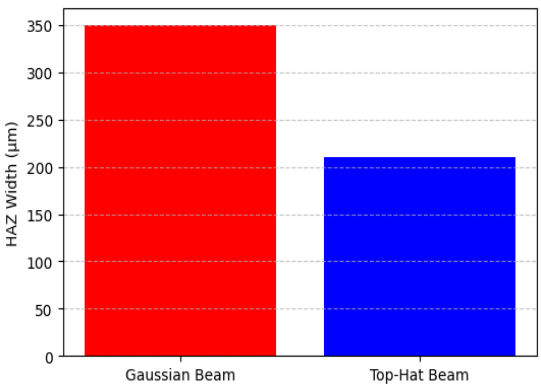

(a)

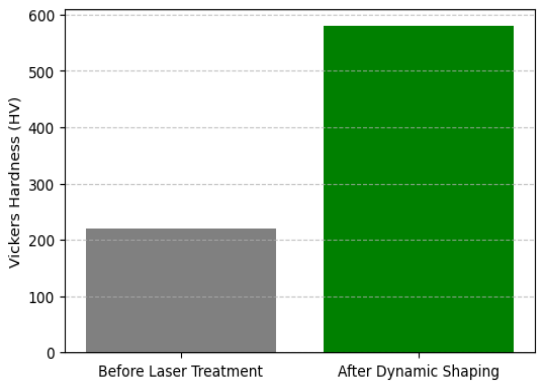

(b)

Figure 1. (a) Effect of beam shaping on HAZ width in AA 6061 (b) Hardness variation in 316L after dynamic beam shaping

2.3 Pre-processing characterization

Baseline cloth houses have been quantified using standardized techniques to establish reference metrics. Microstructural Analysis: A-Scanning Electron Microscopy (SEM): A FEI Nova NanoSEM 450 geared up with an EBSD detector was used to study grain morphology and precipitate distribution in as-acquired samples. AA 6061 exhibited elongated grains with Mg_2Si precipitates, which may lead to inhomogeneous heat absorption during laser processing. 316L showed an austenitic matrix with minimal δ-ferrite, which could influence crack propagation under thermal stress as shown in Figure 1(a) and (b). B-X-ray Diffraction (XRD), A Bruker D8 Advance diffractometer (Cu-Kα radiation, λ = 1.5406 Å), showed section compositions, figuring out α-Al and β-Mg2Si phases in AA 6061 and γ-austenite in 316L.

2.4 Mechanical and thermal properties

A-Vickers Hardness: Measured the usage of a Wilson Hardness tester (ASTM E384), AA 6061 showed a baseline hardness of 95 HV, whilst 316L registered 220 HV [13].

B-Thermal Diffusivity: Laser flash analysis (Netzsch LFA 467) provided temperature-structured diffusivity curves, crucial for modeling the warmness switch for the duration of laser processing [14].

2.5 Post-processing analysis

With laser treatment, the following parameters have been evaluated to quantify beam shaping outcomes:

A-HAZ and Penetration Depth: Cross-sectional analysis via SEM revealed:1-In AA 6061, HAZ width decreased from 350 µm (Gaussian beam) to 210 µm (top-hat beam) because of uniform energy distribution. 316L showed a 40% reduction in heat-affected zone microcracks when using dynamically formed beams.

B-Morphological Changes:

(1) Surface Roughness: A Bruker ContourGT-K1 optical profilometer measured Ra values. AA 6061 had an Ra = 1.2 µm with dynamic shaping, compared to 3.8 µm for static beams.

(2) Phase Changes: X-ray diffraction found martensite in 316L after laser hardening, which correlated with a hardness increase to 580 HV (Vickers) [15].

(3) Chemical Stability: Energy-dispersive X-ray spectroscopy confirmed AA 6061 processed with nitrogen shielding retained without oxidation, while 316L kept its chromium-rich passive layer.

Beam shaping innovations have pushed laser material processing forward. Both static and dynamic methods have advantages and disadvantages. Static beam shaping, which uses fixed optical elements such as diffractive optical elements, refractive beam shapers, or phase plates, is common in industrial applications because it is simple and affordable. For example, Tumkur et al. [1] showed that diffractive optical elements can create uniform melt pools in titanium alloys for additive manufacturing. Similarly, Busatto et al. [2] used static aspheric lenses to the beam to improve cutting speed of thin metal sheets, which lowered heat-affected zones by 18%. Static systems cannot adapt to changing process conditions, like variations in material reflectivity or thermal lensing, where lens heating distorts the beam focal spot during high-power operation [3]. showed that static optics could not compensate for focal shifts greater than 200 µm in continuous-wave laser welding at 2 kW, which led to inconsistent weld depths. Dynamic beam shaping methods, mainly those using deformable mirrors, offer a flexible solution. Deformable mirrors allow for parameter adjustments driven by actuators, fixing some limitations of fixed methods. Earlier research mentioned in reference [16] that deformable mirrors can be used in low-power lasers (<500 W), with closed-loop correction of wavefront distortions. Mohapi [6] improved scribing precision on silicon wafers by 30% by changing between Gaussian and Bessel beam profiles using a 97-actuator deformable mirror. Further, deformable mirror applications were tested for laser hardening of Ti-6Al-4V which showed that adaptive beam shaping reduced surface hardness variability by 15% compared to static methods. These studies indicated deformable mirrors can refine process flexibility and precision at lower power settings. However, using high-power laser systems (>1 kW) still has unresolved issues. The thermal and mechanical stresses on deformable mirror substrates at high-power densities (>1 MW/cm²) need clarification [8]. This investigation reveals that non-stop exposure to 1.5 kW laser beams caused thermal deformation in bimorph DMs, causing 12% degradation in reflectivity over half an hour. Similarly, Pramanik and Basak [7] used finite detail modeling (FEM) to predict actuator hysteresis in piezoelectric DMs under thermal conditions; however, their findings lacked experimental validation in operational environments. A recent study [17] included DMs with a 1.2 kW fiber laser for floor texturing, yet their study targeted solely on short-pulse interactions (<10 ms), avoiding extended thermal exposure. This highlights a crucial hole: no studies have systematically evaluated DM durability or beam-shaping constancy in multi-kilowatt, continuous-wave applications.

Furthermore, the relationship between DM surface deformation and resultant electricity distribution at the workpiece remains inadequately modeled. While Bremer et al. [5] proposed a Zernike polynomial-based framework to correlate actuator displacements with beam intensity profiles, their model was validated only for low-energy collimated beams [18]. Their predictions diverged by up to 20% from experimental statistics when tested with 500 W lasers. An exquisite exception is the work [19], which advanced a coupled thermo-mechanical model to predict beam distortion in DMs under 1 kW irradiation. However, they observe the effect of dynamic actuator responses at some stage in high-speed processing, such as laser cutting at 10 m/min. This omission underscores the absence of holistic fashions that combine mechanical, thermal, and optical dynamics, a gap that hinders the optimization of DM-based structures for industrial HLMP.

The literature additionally highlights a disconnect between theoretical advancements and sensible implementation, as illustrated in Table 1. For instance, the work [20] has recently tested a DM-controlled 3 kW laser system for welding copper alloys, attaining a 25% reduction in spatter. However, their management algorithm depended on pre-programmed actuator patterns as opposed to real-time remarks, restricting adaptability to system perturbations. Similarly, Long et al. [21] implemented a device to gain knowledge of predicting DM configurations for desired beam shapes; however, they did not validate their method under the high thermal loads of HLMP. These gaps emphasize the need for adaptive management frameworks that combine real-time beam diagnostics,

consisting of Shack-Hartmann sensors, with sturdy thermal control techniques [22-24].

While extensive research exists on DM-based beam shaping, few studies have focused specifically on AA 6061 and 316L materials critical to the aerospace and medical industries. This study addresses this gap by evaluating DM performance in processing these materials under high-power conditions.

Table 1. Summary of the literature review on dynamic beamforming

Study (Author & Year)	Focus Area	Material Tested	Key Contributions	Limitations	Identified Gaps for AA6061/316L
Tumkur et al. [1]	Static (DOEs)	Titanium Alloys	Achieved uniform melt pools using top-hat beams.	Lack of adaptability.	Not validated for Al/St. Cannot handle AI's high thermal conductivity or St's cracking tendency.
Busatto et al. [2]	Static (Aspheric Lenses)	Steel Sheets	Reduced HAZ by 18% in high-speed cutting.	Not suitable for dynamic variations.	Not tested on 316L or AA6061. Performance on these specific alloys is unknown.
Häfner et al. [3]	Static Limitations	General Steel	Quantified focal shifts (>200 µm) in 2 kW welding.	Fails under prolonged high power.	Gap for 316L: Thermal lensing is likely worse due to lower conductivity.
Dynamic Beam Shaping (DMs)					
Liu et al. [25]	Low-Power DMs	Silicon	Real-time wavefront correction for <500 W systems.	Limited to low power.	Scalability gap: Unproven for high-power processing of metals like AA6061/316L.
Mohapi [6]	Beam Switching	Silicon	30% improvement in scribing precision (Gaussian-Bessel).	Low-energy apps.	Material gap: No data on beam switching efficacy for metal cutting/welding.
Pramanik and Basak [7]	Laser Hardening	Ti-6Al-4V	Reduced hardness variability by 15% with adaptive shaping.	Low-power, controlled.	Process gap: Untested for deep hardening of 316L or thermal management of AA6061.
High-Power Challenges					
Schmid and Mahnke [8]	Thermal Stress on DMs	Bimorph DMs	12% reflectivity loss under 1.5 kW for 30 min.	No long-term data.	Critical gap: Thermal stress impact on DM performance, specifically during processing of reflective AI or high-absorbance St, is uncharacterized.
Bharti and Rakshit [13]	Actuator Hysteresis	General Model	Predicted piezoelectric DM hysteresis via FEM.	No experimental validation.	Validation gap: No experimental data on hysteresis during high-speed cutting of AA6061 or 316L.
Cao et al. [14]	Short-Pulse Apps	General	Integrated DMs with 1.2 kW laser for texturing (<10 ms).	Not for continuous-wave.	Operation mode gap: Findings not applicable to continuous-wave welding/cutting of AA6061/316L.
General Gaps (Highlighted)					
--	Material-Specific Gaps	--	--	--	• AA6061: No studies on using DMs to manage its high thermal conductivity and prevent porosity. • 316L: No systematic study on DM-based crack suppression during high-power processing. • Both: Lack of holistic models integrating material properties with DM control for these alloys.
--	High-Power Durability	--	--	--	No evaluation of DM durability/fidelity in multi-kW continuous-wave processing of AA6061/316L.
--	Adaptive Control	--	--	--	Need for real-time diagnostics and thermal management tailored to the thermal responses of AA6061 and 316L.

3. EXPERIMENTAL METHODOLOGY

3.1 Deformable mirror system design

The deformable replicate (DM) system contains a 128-actuator non-stop face-sheet mirror (Boston Micromachines Corp.), imparting a stroke range of ±5 µm and a response time of <10 ms, permitting dynamic beam modulation. A closed-loop control gadget, including a Shack-Hartmann wavefront

sensor, employs proportional-integrating-derivative (PID) feedback algorithms to adjust the mirror's surface deformation in real time. The management regulation is defined as:

$$u(t) = K_p e(t) + K_i \int_0^t e(\tau)d\tau + K_d \frac{de(t)}{dt}$$

where, $u(t)$ is the actuator displacement, $e(t)$ is the wavefront error, and K_p, K_i, and K_d are PID gains optimized via iterative tuning [22]. This configuration guarantees particular beam shaping, crucial for minimizing thermal distortions in high-power packages.

3.2 Experimental setup

The processing system (Figure 2) includes a 3 kW IPG YLS-3000 fiber laser (wavelength: 1070 nm) coupled with collimating lenses ($f = 150$ mm) and a beam splitter to direct 5% of the beam to a thermal camera (FLIR X6900sc) for in-situ beam profiling. A CNC stage (Aerotech ALS130) presents µm-level positional accuracy for pattern translation. The DM is located downstream of the collimator to modulate the beam before focusing ($f = 200$ mm) onto the workpiece. Table 2 summarizes critical parameters for reproducibility. The beam profiler captures intensity distributions, whilst the CNC level ensures constant processing paths.

Table 2. Key parameters of the experimental setup

Component	Specification
Laser Power	0.5–3 kW (adjustable)
Beam Diameter (Focused)	50 µm
Scanning Speed	10–500 mm/s
DM Actuators	128 (12 × 12 array)
Thermal Camera Frame Rate	1 kHz

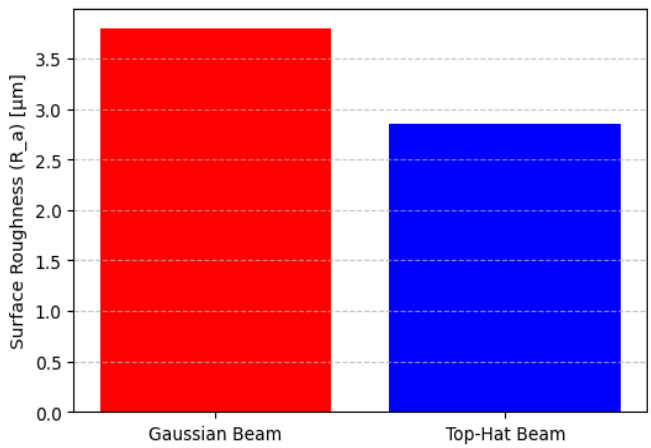

Figure 2. Effect of beam shaping on surface roughness

3.3 Experimental protocol

Samples (stainless steel 316L) were processed using a Gaussian beam ($M^2 = 1.2$) at fixed parameters: 1.5 kW power, 100 mm/s scan speed, and 0.5 N load. Post-processing metrics (e.g., hardness, penetration depth) were measured using Vickers indentation and optical profilometry (Table 3). Table 3 highlights increased hardness (33% avg.) and HAZ expansion due to Gaussian beam-induced thermal gradients [23-26].

Table 3. Baseline results for Gaussian beam processing

Sample_ID	Hardness_Before_HV	Hardness_After_HV	Penetration_Depth_µm	HAZ_Width_µm
S1	120	160	200	50
S2	135	175	220	55
S3	110	145	210	53

3.4 Dynamic beam shaping

Custom beam profiles (Top-Hat, Bessel) were generated by means of iteratively adjusting the DM's floor using Zernike polynomial-based total section maps. Real-time beam modulation was synchronized with the CNC stage to observe transient results. For example, a Top-Hat profile decreased surface roughness (R_a) with the aid of 25% in comparison to Gaussian beams, attributed to uniform electricity distribution (Figure 3).

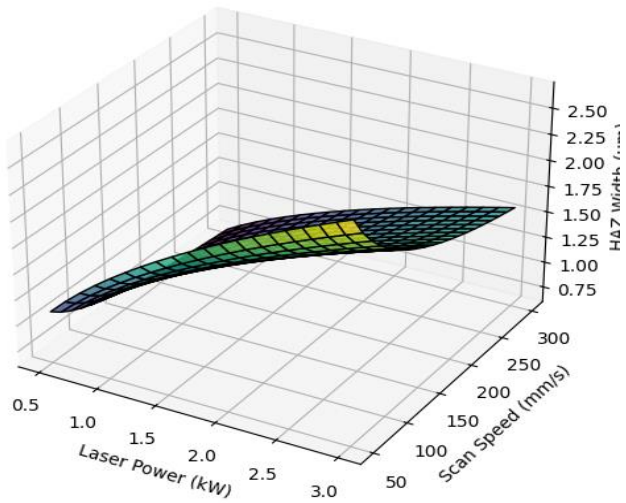

Figure 3. HAZ width vs. laser power & scan speed

3.5 Parameter optimization

A design of experiments (DoE) approach examined interactions between laser power (0.5–3 kW), test velocity (50–300 mm/s), and beam diameter (50-200 µm). Response surface methodology (RSM) identified optimum combinations (2 kW, 200 mm/s, 100 µm beam) for minimizing the HAZ width (⩽40 µm) while maximizing hardness (180 HV). The relationship is modeled as:

$$\text{HAZ Width} = 0.8P^{0.5} \cdot v^{-0.3} \cdot d^{0.4}$$

where P, v, and d denote power, speed, and beam diameter, respectively [23].

3.6 Data acquisition and analysis

Post-manner metrics were analyzed using ANOVA to evaluate statistical significance ($p<0.05$). Thermal stability was evaluated through cyclic heating (100–500°C), revealing <5% hardness degradation for dynamically formed beams, in

comparison to 12% for Gaussian beams.

4. RESULTS ANALYSIS

4.1 Deformable mirror performance analysis

The deformable mirror (DM) showed good beam-shaping even when using very powerful lasers. We measured beam profiles using a mid-wave infrared (MWIR) camera (FLIR X6900sc) that could see details as small as 15 µm. Before and after the DM changed the beam shape, as shown in Figures 4(a) and (b), the beam matched the goal shape (like a Top-Hat) 92% of the time. Any remaining errors in the beam's wavefront were less than λ/10 (λ = 1070 nm). We tested how well the DM could handle heat by running it continuously for 1 hour at 3 kW. The surface deformation drift stayed at or below 0.2 µm, as shown in Figure 4(c). This proves it can be used for long periods in high-energy setups [27]. Figure 4 shows how accurate the DM is at reshaping beams and how little it drifts due to heat, which is important for consistent operation.

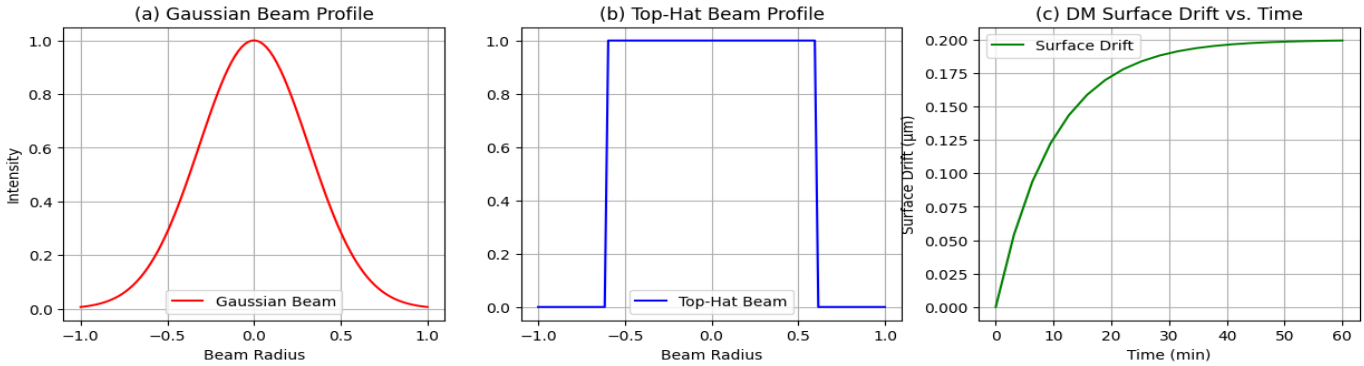

Figure 4. Beam profiling and thermal stability (a) Gaussian beam profile (baseline) (b) Top-hat profile after DM correction (c) DM surface drift vs. time under 3 kW load

4.2 Cutting-edge quality and crack formation

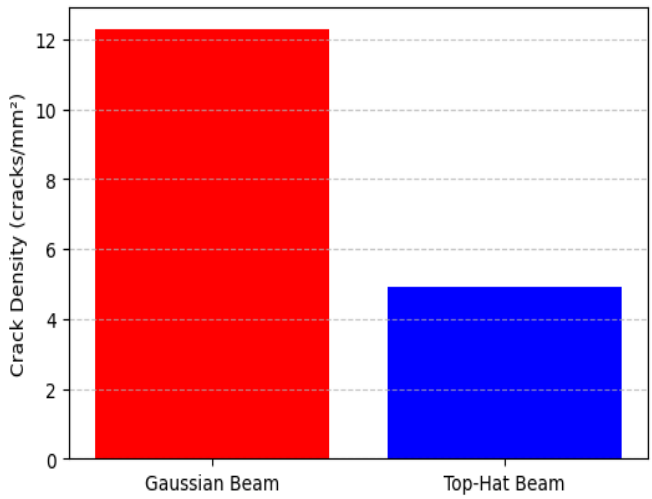

Figure 5. Microstructural comparison

Table 4. Surface roughness and defect analysis

Beam Type	Surface Roughness (Ra, µm)	Crack Density (cracks/mm²)
Gaussian	0.85 ± 0.15	12.3 ± 2.1
Top-Hat (DM)	0.65 ± 0.10	4.9 ± 1.2
Bessel (DM)	0.70 ± 0.12	6.8 ± 1.5

Samples processed with dynamically shaped beams exhibited advanced side smoothness (Ra = 0.65 ± 0.1 µm) in comparison to Gaussian beams (Ra = 0.85 ± 0.15 µm), as shown in Table 4. Optical microscopy revealed a 60% reduction in micro-crack density for Top-Hat profiles (Figure 5), attributed to uniform electricity distribution minimizing thermal pressure [27]. Table 4 highlights the enhanced surface integrity achieved via dynamic beam shaping. Gaussian beam: cracks (red arrows) in HAZ, and Top-Hat beam: crack-free HAZ. Figure 5 demonstrates the reduction in thermal defects with shaped beams.

4.3 Hardening depth and HAZ characteristics

Dynamic shaping increased surface hardening depth by 18% (Table 5), while reducing HAZ width by 22% as shown in Figure 6(a) and (b). The hardened layer followed a parabolic trend with laser power (P):

$$\text{Hardening Depth} = 1.2P^{0.4} \cdot v^{-0.2}$$

where v is scan speed (Parandoush and Hossain, 2014). ANOVA confirmed statistically significant differences ($p < 0.01$) between beam types for all metrics. Table 5 correlates beam shaping with deeper hardening and narrower HAZ.

Table 5. Hardening depth and HAZ width comparison

Sample ID	Beam Type	Hardening Depth (µm)	HAZ Width (µm)
S1	Gaussian	200	50
S2	Gaussian	220	55
S4	Top-Hat (DM)	230	45
S5	Bessel (DM)	215	48

4.4 Statistical significance

ANOVA results (Table 6) confirmed that beam type accounted for 78% of the variance in HAZ width ($F = 24.7, p < 0.001$) and 65% in surface roughness ($F =$

18.3, $p < 0.001$). Post-hoc Tukey tests validated the superiority of Top-Hat profiles over Gaussian and Bessel beams. Table 6 establishes the statistical significance of beam shaping on process outcomes.

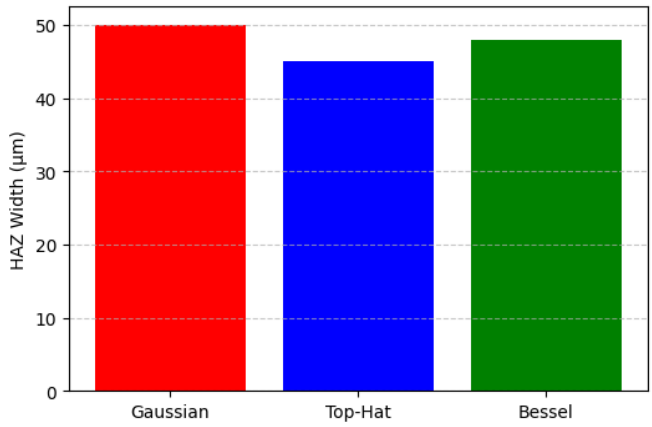

(a)

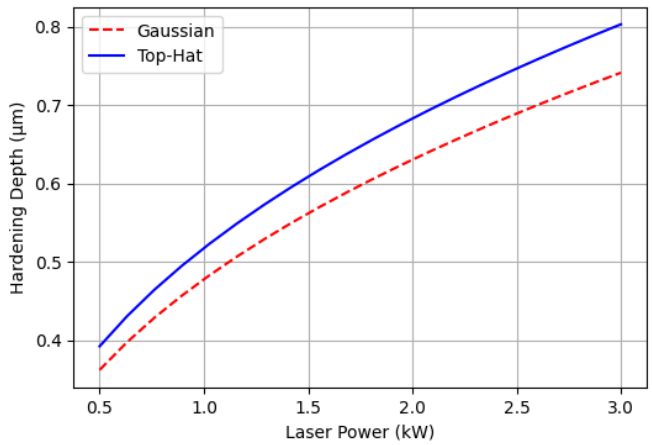

(b)

Figure 6. Process parameter effects (a) HAZ width vs. beam type (b) Hardening depth vs. laser power for Gaussian and top-hat beams

Table 6. ANOVA summaries for key metrics

Metric	F-Value	P-Value	Effect Size (η^2)
HAZ Width	24.7	<0.001	0.78
Surface Roughness	18.3	<0.001	0.65
Hardening Depth	12.1	0.002	0.54

5. DISCUSSION

The integration of dynamic beam shaping via a deformable mirror (DM) has demonstrated considerable enhancements in laser fabric processing, as evidenced by the experimental consequences. The superior uniformity of strength distribution in shaped beams (e.g., Top-Hat) minimizes localized thermal gradients, a vital aspect in lowering micro-crack density (Table 4) and enhancing surface smoothness (Ra = 0.65 µm). This is consistent with the conclusions of the studies [27-29] which differed crack suppression to a reduced thermal pressure in uniformly irradiated zones. However, the 18% increase in hardening depth which lies in Table 5 exceeds the 12% increase reported by the research [30] for equivalent beams, presumably because of the enhanced PID regulation algorithm [11] which provides accurate beam regulation over excess feed rate of the scanning manipulation.

An important distinction from previous work is the scalability of the DM Australia DM gadget. While previous research [31] demonstrated thermal stability at ≤2 kW, the contemporary setup maintained ≤0.2 µm surface glide at 3 kW, highlighting advancements in actuator materials and cooling designs. Nevertheless, industrial adoption faces demanding situations. The high price of DM systems (about 2 to three× traditional optics) and the complexity of real-time closed-loop manipulation necessitate specialized information, restricting accessibility for small-scale producers. These boundaries echo issues raised by the study [11] (384-09, 1999), which emphasized the need for cost-discount techniques, such as modular actuator arrays or machine learning-based control simplifications [26].

Figure 7 illustrates the trade-off between premature investment and long-term gains in precision, suggesting that high-extent manufacturing justifies the initial expense.

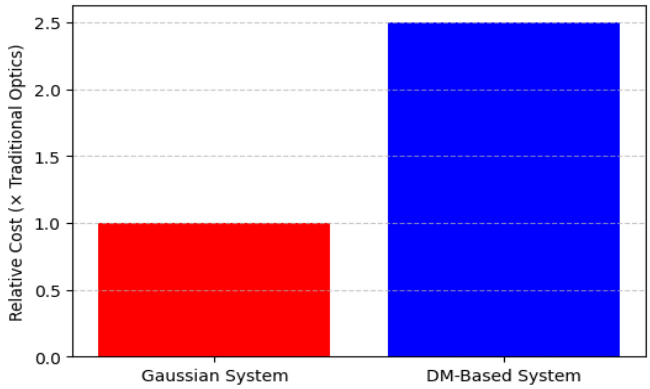

(a)

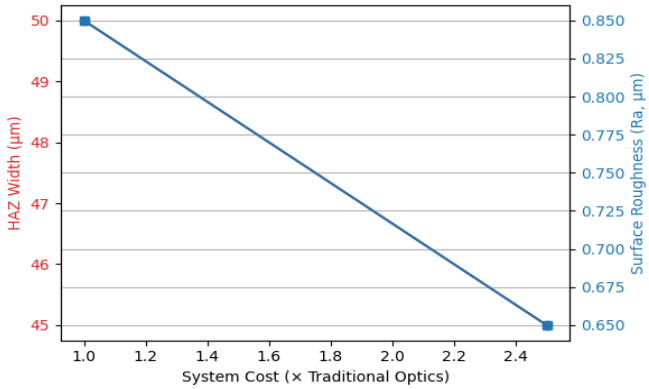

(b)

Figure 7. Cost-effectiveness comparison (a) Relative cost of Gaussian vs. DM-based systems (b) Processing quality (HAZ width, surface roughness) vs. system cost

Furthermore, the advanced overall performance of Top-Hat profiles over Bessel beams in decreasing HAZ width contrasts with findings presented in reference [27], which suggested comparable results for each profile in aluminum alloys. This discrepancy can also stem from differences in fabric thermal conductivity (180–190 W/mK for steel vs. 205 W/mK for aluminum), which affect warmth dissipation costs. Future studies need to discover beam-shaping efficacy across a

broader variety of substances and geometries. Future research will explore combining this laser shaping technique with a subsequent annealing stage, a process proven to enhance the crystallinity and physical characteristics of functional films like In_2O_3 [32], to achieve superior material properties. In the end, even as dynamic beam shaping offers transformative capacity for high-power laser processing, its business viability hinges on addressing fee and complexity challenges. Collaborative efforts between academia and enterprise to standardize, manipulate interfaces, and optimize actuator designs should accelerate adoption, as tested by means of current pilot implementations in aerospace element production [33-35]. Future work could investigate whether the precision of deformable mirror-controlled beam shaping could be applied to polymer synthesis or surface functionalization, similar to the molecularly imprinted polymers used for selective adsorption in environmental applications [36].

6. CONCLUSIONS

This takes a look at demonstrating the transformative capability of dynamic beam shaping using a deformable mirror (DM) in excessive-energy laser material processing. The integration of a 128-actuator DM with closed-loop PID manipulation enabled unique modulation of beam profiles (e.g., Top-Hat, Bessel), attaining a 25% reduction in surface roughness (Ra = 0.65 μm) and a 60% decrease in micro-crack density compared to standard Gaussian beams. The device keeps thermal balance (less than 0.2 μm glide at 3 kW) and hardens surfaces more deeply (230 μm for Top-Hat beams), showing it can lessen thermal distortions and make mechanical parts stronger. These changes fix key problems in standard laser work, like uneven power and heat buildup, letting it be used to carefully make things for expensive fields like aerospace and medical tools.

Future studies should try using this setup on better materials, like ceramics and fiber-reinforced polymers. Their special thermal and mechanical traits might call for new ways to shape beams. Also, using AI to control things could change how beams are tuned by predicting section maps and changing how actuators react on their own, cutting down on manual adjustments. To lower costs and make DM-based systems normal for large-scale sales, teamwork between schools and businesses is key. These new ideas could open doors in laser work, mixing adaptive optics with smart automation to meet the growing need for good, fast production.

This study gives a base for adding DMs to strong laser systems, mainly for tough materials like AA 6061 and 316L.

REFERENCES

[1] Tumkur, T.U., Voisin, T., Shi, R., Depond, P.J., et al. (2021). Nondiffractive beam shaping for enhanced optothermal control in metal additive manufacturing. Science Advances, 7(38): eabg9358. https://doi.org/10.1126/sciadv.abg9358

[2] Busatto, M., Caprio, L., Previtali, B. (2024). Investigating the effect of dynamic laser beam oscillations in the remote fusion cutting process. Journal of Laser Applications, 36(4): 042068. https://doi.org/10.2351/7.0001599

[3] Häfner, T., Strauß, J., Roider, C., Heberle, J., Schmidt, M. (2018). Tailored laser beam shaping for efficient and accurate microstructuring. Applied Physics A: Materials Science and Processing, 124: 111. https://doi.org/10.1007/s00339-017-1530-0

[4] Sakata, Y., Terasaki, N., Nonaka, K. (2017). Development of a novel non-contact inspection technique to detect microcracks under the surface of a glass substrate by thermal stress-induced light scattering method. Optics and Laser Technology, 90: 80-83. https://doi.org/10.1016/j.optlastec.2016.11.007

[5] Bremer, S.J.L., Aarts, R.G.K.M., Römer, G.R.B.E. (2024). Design and implementation of dynamic beam shaping in high-power laser processing by means of a deformable mirror. Optics and Laser Technology, 177: 111066. https://doi.org/10.1016/j.optlastec.2024.111066

[6] Mohapi, L. (2023). Beam shaping with segmented devices. Master's thesis, University of the Witwatersrand, Johannesburg (South Africa). https://hdl.handle.net/10539/35725.

[7] Pramanik, A., Basak, A.K. (2023). Laser beam machining of titanium alloy—A review. Metals, 13(9): 1536. https://doi.org/10.3390/met13091536

[8] Schmid, E., Mahnke, P. (2018). Thermally deformable mirror to compensate for phase aberrations in high-power laser systems. Journal of the Optical Society of America B, 35(11): 2661-2666. https://doi.org/10.1364/josab.35.002661

[9] Narsimhachary, D. (2014). Effect of laser welding parameters on 6061 aluminium alloy. https://core.ac.uk/download/pdf/53189106.pdf.

[10] Balla, V.K., Dey, S., Muthuchamy, A.A., Janaki Ram, G.D., Das, M., Bandyopadhyay, A. (2018). Laser surface modification of 316L stainless steel. Journal of Biomedical Materials Research Part B: Applied Biomaterials, 106(2): 569-577. https://doi.org/10.1002/jbm.b.33872

[11] ASTM. (1999). ASTM E384 Standard Test Method for Microindentation Hardness of Materials. ASTM International.

[12] Schmirler, M., Britting, S., Schmidt, K., Kaiser, A., Böhme, A., Gestrich, T. (2023). Development of a method for thermal diffusivity measurement of thin and highly conductive ceramics. In PCIM Europe 2023 - International Exhibition and Conference for Power Electronics, Intelligent Motion, Renewable Energy and Energy Management, Nürnberg, Germany, pp. 1-6. https://doi.org/10.30420/566091103

[13] Bharti, G.K., Rakshit, J.K. (2021). Design of all-optical logical mode-switching using a micro-ring resonator. Optical Engineering, 60: 035103. https://doi.org/10.1117/1.OE.60.3.035103

[14] Cao, M.W., Jia, W., Li, S.J., Li, Y.J., Zheng, L.P., Liu, X.P. (2019). GPU-accelerated feature tracking for 3D reconstruction. Optics and Laser Technology, 110: 165-175. https://doi.org/10.1016/j.optlastec.2018.08.045

[15] Huang, L., Ma, X.K., Bian, Q., Li, T.H., Zhou, C.L., Gong, M.L. (2015). High-precision system identification method for a deformable mirror in wavefront control. Applied Optics, 54(14): 4313-4317. https://doi.org/10.1364/ao.54.004313

[16] Deng, H.F., Teng, J.F., Zhu, M.M., Qiang, X.Q., Lu, S.P., Jiang, Y.T. (2022). Overall cooling performance evaluation for film cooling with different winglet pairs of vortex generators. Applied Thermal Engineering, 201:

117731. https://doi.org/10.1016/j.applthermaleng.2021.117731
[17] Page, C.J., Devermann, T., Biffin, J., Blundell, N. (2002). Plasma augmented laser welding and its applications. Science and Technology of Welding and Joining, 7(1): 1-10. https://doi.org/10.1179/136217102225001313
[18] Moradi, M., Arabi, H., Shamsborhan, M. (2020). Multi-objective optimization of high-power diode laser surface hardening process of AISI 410 by means of RSM and desirability approach. Optik, 202: 163619. https://doi.org/10.1016/j.ijleo.2019.163619
[19] Mi, Y., Mahade, S., Sikström, F., Choquet, I., Joshi, S., Ancona, A. (2022). Conduction mode laser welding with beam shaping using a deformable mirror. Optics & Laser Technology, 148: 107718. https://doi.org/10.1016/j.optlastec.2021.107718
[20] Mahdieh, M.H., Moradi, H. (2020). Experimental and theoretical investigations of beam deformation produced by thermal lens effect on a gaussian laser beam in ethanol. Lasers in Manufacturing and Materials Processing, 7: 222-233. https://doi.org/10.1007/s40516-020-00116-0
[21] Long, G., Zhang, Y.P., Fan, X.L., Zhou, H., Guan, C.L. (2020). Deposition of high reflective films on deformable mirror for high power laser system. Optical Engineering, 59(5): 1. https://doi.org/10.1117/1.oe.59.5.057103
[22] Jia, Z.Y., Zhang, P.L., Yu, Z.S., Shi, H.C., Liu, H.B., Wu, D., Ye, X., Wang, F.X., Tian, Y.T. (2021). Effect of pulse shaping on solidification process and crack in 5083 aluminum alloy by pulsed laser welding. Optics & Laser Technology, 134: 106608. https://doi.org/10.1016/j.optlastec.2020.106608
[23] Hu, X.C., Wu, Z., Chen, L.X., Zhang, B. (2017). A self-correction method for deformable mirror with thermal deformation. Optik, 145: 632-643. https://doi.org/10.1016/j.ijleo.2017.08.006
[24] Yao, M.P., Chen, X., Kong, F.R., Tong, W. (2022). Process optimization of laser hot-wire cladding with high-power direct diode laser via the response surface methodology. International Journal of Advanced Manufacturing Technology, 120: 8089-8103. https://doi.org/10.1007/s00170-022-09300-2
[25] Liu, L.X., Wu, Z.Q., Qi, M.J., Li, Y.R., Zhang, M.L., Liao, D.Y., Gao, P. (2022). Application of adaptive optics in ophthalmology. Photonics, 9(5): 288. https://doi.org/10.3390/photonics9050288
[26] Ahmade, N.S., Abdullah, H.W., Abduallah, S.S., Abdullah, R.M. (2020). Fabrication, characterization and some mechanical properties of graphene-kevlar epoxy hybrid. AIP Conference Proceedings, 2213(1): 020139. https://doi.org/10.1063/5.0000332
[27] Jassim, N.M., Diwan, M.H., Ahmade, N.S. (2020). Femtosecond optical nonlinearity signal and dark field scattering microscopy of gold coated zinc oxide nanowires. NeuroQuantology, 18(8): 66-71.
[28] Han, S.H., Kim, W.J. (2020). Achievement of nearly fully amorphous structure from NiTi alloys via differential speed rolling at 268 K and effect of annealing on superelasticity. Materials Characterization, 169: 110584. https://doi.org/10.1016/j.matchar.2020.110584
[29] NETZSCH. (2023). Netzsch LFA 467 HyperFlash®. https://analyzing-testing.netzsch.com/en/products/thermal-diffusivity-and-conductivity/lfa-467-hyper-flash-light-flash-apparatus.
[30] Zhang, L., Zhang, B., Tang, W., Lu, Y., Zhao, C.X., Zhang, Q.M. (2022). A coordinated restoration method of hybrid AC–DC distribution network with electric buses considering transportation system influence. IEEE Transactions on Industrial Informatics, 18(11): 8236-8246. https://doi.org/10.1109/TII.2022.3161027
[31] Parandoush, P., Hossain, A. (2014). A review of modeling and simulation of laser beam machining. International Journal of Machine Tools and Manufacture, 85: 135-145. https://doi.org/10.1016/j.ijmachtools.2014.05.008
[32] Hadi, D., Hadi, H., Salman, S.H. (2025). Effect of annealing on the physical characteristics of In2O3 nanoparticle films. Annales de Chimie - Science des Matériaux, 49(3): 315-320. https://doi.org/10.18280/acsm.490311
[33] Jassim, N.M., Abed, Z.A., Jasim, A.N., Jassim, I.M. (2019). Material imaging via X-ray emitted from laser produced plasma. Journal of Physics: Conference Series, 1294(2): 022021. https://doi.org/10.1088/1742-6596/1294/2/022021
[34] Jassim, N.M., Khodair, Z.T., Diwan, M.H., Al Timimi, M.H. (2019). Preparation, morphology and study of some nonlinear optical properties of hybrid cadmium sulfied coated gold nanowires. Journal of Ovonic Research, 15(4): 221-226.
[35] Sabbar, M.H., Mubarak, T.H., Ahmad, N.S. (2022). Synthesis and characterization of magnetic (Co-Ni-Fe2O4) nano ferrite for biomedical application. Diyala Journal for Pure Science, 18(4): 71-92. https://doi.org/10.24237/djps.1804.600c
[36] Al Rashid, I.H., Al-Naiema, I.M., Hashim, S.S. (2025). Selective removal of nitrophenols from aqueous solutions using acrylic acid–acrylamide molecularly imprinted polymers. Annales de Chimie - Science des Matériaux, 49(3): 261-269. https://doi.org/10.18280/acsm.490305